Microbiome variation during culture growth of the European house dust mite, *Dermatophagoides pteronyssinus*

Marta Nesvorna
Crop Research Institute
Vit Molva
Crop Resrarch Institute
Stano Pekar
Masarykova Univerzita
Elena Shcherbachenko
Crop Rsearch Institute
Tomas Erban
Crop Research Institute
Stefan J Green
University of Illinois at Chicago
Pavel Klimov
University of Michigan
Jan Hubert (hubert@vurv.cz)
Crop Research Institute https://orcid.org/0000-0003-0740-166X

Research

Keywords: House dust mite, Spent growth medium, Feeding, Malassezia

Posted Date: March 19th, 2020

DOI: https://doi.org/10.21203/rs.3.rs-18047/v1

Version of Record: A version of this preprint was published at FEMS Microbiology Ecology on March 1st, 2021. See the published version at https://doi.org/10.1093/femsec/fiab039.

Abstract

Background: The house mite *Dermatophagoides pteronyssinus* is an important allergen source. In mite cultures used for anti-allergic vaccine production, both mite population growth patterns and microbiome composition can affect the level of allergen production. Here we analyzed mite microbial communities: “internal community” inside mites (ingested) and “environmental community” from culture environment) and their temporal changes during mite culture growth. To explain the microbiome temporal changes in mites and mite culture, the microbial profiles were correlated to the concentration of mite nitrogenous waste products (*i.e.*, guanine) and mite population density.

Results: The population dynamic of *D. pteronyssinus* showed a nonlinear humped-shaped pattern during mite culture growth, and a nonlinear pattern was also observed for the mite nitrogenous waste product guanine. Mite microbial communities were remarkably consistent between replicates within the same treatment and composed of relatively few dominant taxa – 11 bacterial and 3 fungal OTUs. Significant changes over time in microbial community structure in the bulk culture environment and internal mite microbiome were observed. The yeast *Saccharomyces cerevisiae,* which is a main component of the yeast extract used in the mite diet, gradually disappeared during the mite culture growth and was replaced by operational taxonomic units derived from the genera *Aspergillus* and *Candida* in both the internal mite community and the environment culture samples. In the ingested community, an OTU derived from the putative fungal pathogen *Malasszia* was detected at low relative abundance. In internal mite community, the relative abundance of bacteria from the genus *Kocuria* positively correlated with mite density but negatively correlated with guanine content. The relative abundance of the bacteria *Virgibacillus pantothenticus* was negatively correlated with mite density in the internal community. In the culture environment, the bacterial species *Lactobacillus fermentum* and yeast *S. cerevisiae* were present in high abundance in diet, but a significant negative relationship with guanine was observed. The fungal taxa *Aspergillus penicillioides* and *Candida mucifera* increased with the amount of guanine in the culture.

Conclusion: The temporal changes in the internal and environmental microbiomes of the *D. pteronyssinus* culture are related to mite population density and guanine contents. The detection of an OTU derived from fungi of the genus *Malassezia* suggests that mites could serve as vectors for dissemination. The dominant bacterial species observed here were Gram-positive bacteria, indicating a limited source for potential vaccine contamination by endotoxins (heat-stable lipopolysaccharides produced mostly by Gram-negative bacteria) in the experimental design used in this study.

Background

Two species of dust mites, Dermatophagoides pteronyssinus and Dermatophagoides farinae, are the major source of allergens in human houses [1]. These organisms are known to produce from 23 to 33 distinct compounds with allergen reactivity as listed on the official WHO/IUIS Allergen Nomenclature Sub-Committee website [2]. These allergens include lipid-binding proteins (Der p 7 and 14), digestive enzymes such as proteases (Der p 1, 3, 6, and 9) and amylase (Der p 4), and antibacterial proteins (lytFM) [3]. From

a quantitative standpoint, the most significant mite allergens are produced through defecation. According to a recent analysis of D. pteronyssinus feces, the compounds Der p 1, 2, 6, 9 and 15 are most abundant in fecal extracts [4], and these proteins could influence the structure of microbial communities in the mite culture environment. In laboratory settings, mites are mass reared to produce allergen extracts for allergy diagnostics and therapeutic treatment [5]. However, allergen extracts can be contaminated by endotoxins – heat stable lipopolysaccharides derived from Gram-negative bacteria [6, 7] that are capable of interacting with the human immune system. Moreover, production of allergens in mite cultures can be influenced by the presence of various microorganisms [8, 9]. Recent studies have indicated that different species or even populations of allergen-producing mites [7, 10] differ in microbiome composition, and that this can be correlated to different expression of known allergens. For example, the expression of several allergens (groups 4, 7, 10, 11, 13, 20 and 36) correlated with the presence of common intracellular bacterial symbionts Wolbachia and Blattabacterium-like bacteria in the mite species Tyrophagus putrescentiae [10].

The microbiome of house dust mites has been recently characterized using deep sequencing of 16S ribosomal RNA (rRNA) gene amplicons [7, 11–14]. These analyses have been performed because importance of mite-associated bacteria in symbiosis and in allergen production has been demonstrated in studies employing antibiotics (e.g, 10% ampicillin), where antibiotics strongly reduced both bacterial abundance and endotoxin content in D. farinae [7]. General microbiome analyses consistently demonstrate that the microbial community of D. farinae is significantly different from that of D. pteronyssinus, and that the difference is primarily due to the presence of intracellular bacteria of the genus Cardinium in D. farinae only [11]. More recently, however, members of a Korean strain of D. farinae were without Cardinium but had an elevated proportion (30% relative abundance) of Gram-negative Bartonella-like bacteria [13]. In other studies of D. farinae and D. pteronyssinus, Bartonella-like bacteria were detected only occasionally [7, 14]. The internal microbiome of the Korean D. pteronyssinus was composed largely of the Proteobacterial species Klebsiella pneumonia, Klebsiella granulomatis, and Rhizobium multihospitum, while Czech laboratory and industrial strains were dominated by bacteria from the genera Kocuria (Actinobacteria) and Staphylococcus (Firmicutes) [14]. In addition to differences in microbiome by mite species, temporal fluctuations in microbial community composition have been observed in both D. farinae and D. pteronyssinus [14]. Interrogation of mite-associated fungal microbiomes has also been performed using cultivation-independent sequence analysis of 18S rRNA gene amplicons. Fungal microbiomes of D. pteronyssinus were dominated by fungi from the taxa Aspergillus penicillioides, Saccharomyces cerevisiae, Wallemia, and Candida. As with bacteria, a succession in fungal communities was detected: the yeast S. cerevisiae was abundant in young mite cultures while other fungal taxa, A. penicillioides and Candida, were abundant in older cultures [14]. Taken together, these studies indicate that the microbiomes of house dust mites are affected by the mite species, mite population (rearing strain), and culture age.

Mite cultures used for allergy extract production show a specific growth pattern, including a lag phase with slow growth of the mite population, followed by exponential growth, and then a final decline phase, when mite populations decrease in abundance and die [15]. The exponential growth stage is most

commonly employed for extract production [5, 16, 17]. We hypothesize that the phases of exponential population growth or decline can be related, either directly or indirectly, to changes in communities of associated microorganisms. Indeed, significant differences in microbial profiles in young and old mites cultures have been observed [14]. However, the same culture was not continuously sampled throughout the duration of the experiment and separate cultures/colonies were sampled at each time point, a sampling methodology that can introduce bias [14].

The objective of this study was to characterize temporal shifts in the structure of the D. pteronyssinus culture microbiome. In this study, we used a continuous sampling design to obtain mites from the same flasks during the entire experiment. As the mite-associated microbiome is different from that of the bulk culture medium, we used two sampling strategies, including: (i) surface sterilization of mites to obtain the mite internal microbiome and (ii) culture rearing medium and feces of mites to obtain the “environmental” culture microbiome. In our analyses, we focused on the relationship between the observed microbial community structure and mite population density, total microcosm respiration, and the nitrogenous waste product guanine. Guanine, the major mite nitrogenous waste product [18–20], has been used as a hygienic index of mite activity in house dust [21], and has been positively correlated with the numbers of mites [22]. In addition to guanine, which could influence the microbial communities in mite rearing systems, the mites themselves are known to alter microbial community structure and activity through grazing [23, 24]. We hypothesize that both the concentration of nitrogenous waste product and mite population density influence microbial community structure.

Results

Mite culture growth, respiration and waste

During D. pteronyssinus culture growth, mite density changes were significantly nonlinear (GAMM-g, $F_{4.9}$ = 597.9, P < 0.0001), and showed a humped-shaped pattern (Fig. 1A). Exponential growth occurred approximately during the first 60 days, followed by a peak lasting about 10 days at an average population of approximately 2,200 individuals per g of diet, with an exponential decline afterwards. The experiment was terminated after 84 days when the mites were not moving, and dead bodies appeared in the culture. The relationship between guanine concentration in the culture environment (mite nitrogenous waste metabolite) and time was also significantly nonlinear (GAMM, $F_{4.9}$ = 412.6, P < 0.0001, Fig. 1B). Guanine concentration increased exponentially during the first 45 days, reached a maximum of about 2,600 $\mu molL^{-1}$, and then declined to about 2,400 $\mu molL^{-1}$. The amount of guanine inside mites near the beginning of experiment (14 days) did not significantly differ from that of mites in the decline phase (84 days) (ANOVA, $F_{1,18}$ = 2.7, P = 0.12) (Additional file 1: Figure S1). Mite gut contents were examined during the course of the experiment, and in addition to diet material that was present in specimens from the all sampled time intervals, the gut contents had fragmented fungal mycelia and spores (Additional file 1: Figure S2). The dietary material itself contained fragmented pieces of plant material (Additional file 1: Figure S2AE), fragmented mycelium (Additional file 1: Figure S2B) and fungal spores (Additional file 1:

Figure S2CD). The presence of dietary material in the gut of the mites sampled during the decline phase indicated that despite the reduced population size, the mites were still alive during the culture decline. Although respiration over time in the microcosms was significantly non-linear (GAM-g, $F_{4.8} = 12.9$, $P < 0.0001$, Fig. 1C), respiration, unlike mite growth and guanine production, had a fluctuating pattern, with peaks at 30 and 70 days.

Factors influencing the composition of bacterial and fungal microbiome in the mite culture

Deep amplicon sequencing was performed on bacterial 16S rRNA gene amplicons and fungal 18S rRNA gene amplicons generated from DNA extracted from six independent flasks. For bacterial amplicons, the average numbers of read per sample was 28,292 (max = 35,507 and min = 11,000) for internal mite community, 17,547 (max = 32,573 and min = 7,407) for environmental culture, and 4,303 (max = 5,687 and min = 3,046) for pasteurized rearing diet (HDMd). The bacterial microbiome was primarily comprised of 11 $OTUs_{97}$, which represented 93.5% of all reads in all treatments. For fungal amplicons, the average numbers of reads per sample was 19,361 (max = 37,235 and min = 2,462) for internal mite community, 26,506 (max = 43,245 and min = 5,571) for environmental culture and 16,138 (max = 27,305 and min = 3,221) for pasteurized rearing diet (HDMd). The fungal microbiome was primarily comprised of 3 $FOTUs_{97}$, which represented 99.0% of all reads in all treatments.

The structure of the microbial community (Additional file 2: Tables S2 and S3) was affected by the culture time (PERMANOVA: Bacteria, $F = 5.8$, $P < 0.0001$; Fungi, $F = 14.2$, $P < 0.0001$) and significantly differed between the internal mite and environmental samples (PERMANOVA: Bacteria, $F = 12.7$, $P < 0.0001$, Fig. 2; Fungi, $F = 9.6$, $P < 0.0001$, Fig. 3). The interaction of the culture development time and source (internal mite/environmental) was also significant (PERMANOVA: Bacteria, $F = 7.1$, $P < 0.0001$; Fungi, $F = 7.1$, $P < 0.0001$). Nonmetric multidimensional scaling (NMDS) showed different patterns of separation between the ingested and environmental culture samples for fungi and bacteria (Fig. 4). The environmental and internal mite samples were clearly distinguished from each other by their bacterial communities along the first two NMDS axes, confirming the results of the PERMANOVA test (Fig. 4AB). Conversely, the internal mite samples showed higher variability along the first two NMDS axes, and the environmental and internal samples largely overlapped (Fig. 4CD) for both bacterial and fungal communities. No significant differences in the microbial profiles between rearing chambers was observed (PERMANOVA: Bacteria, $F = 0.8$, $P = 0.64$; Fungi, $F = 1.0$, $P = 0.34$), indicating that microbial communities in the mite culture studies were similar in all experimental flasks, and similar trajectories of microbial communities over time were observed.

Bacterial microbiome

Alpha diversity metrics were calculated for internal mite bacterial communities and the external house dust mite rearing diet (HDMd) bacterial community at the level of OTUs. The vast majority of bacterial

diversity in both sample types was composed of 11 OTU-at 97% similarity (Fig. 2AB). The diversity (Simpson's diversity index) of the internal bacterial community showed significant oscillations over time (GAMM, $F5.9 = 10.7$, $P < 0.0001$, Fig. 5A), with peaks close to 30 and 55 days. Conversely, the diversity of the external bacterial community had a significant asymptotic increase with time (GAMM, $F4.3 = 58.9$, $P < 0.0001$, Fig. 5B), with the greatest increase observed during the first 30 days of growth.

The internal mite bacterial community was largely composed of four OTUs, including Staphylococcus sp. (OTU_3), Kocuria sp. (OTU_1), a Virgibacillus pantothenticus (OTU_4), and Burkholderia contaminans (OTU_7). Of these four OTUs, Staphylococcus and Kocuria OTUs were dominant. The relative abundance of these and other more minor taxa fluctuated during the course of the study with, for example, the relative abundance of OTU_4 V. pantothenticus and OTU_7 B. contaminans highest during the 14 to 56 day period and nearly absent before and after this time period.

A unidirectional shift in bacterial environmental community structure over time was observed in the house dust mite rearing diet (HDMd). Initially, the HDMd was almost entirely composed of Lactobacillus fermentum (OTU6), which disappeared after 28 days of culture growth. By day 14, some internal mite bacteria could be detected in the HDMd, including Staphylococcus sp. (OTU_3), Kocuria sp. (OTU_1), and V. pantothenticus (OTU_4). From 42–56 days, the Staphylococcus sp. (OTU_3) was the most abundant taxon observed, while V. pantothenticus (OTU_4) became the most abundant taxon in the 70 to 84-day samples. Declining (84-day old) environmental samples were characterized by high Oceanobacillus arenosus (OTU_8) and Lentibacillus massiliensis (OTU_9) abundances, which were at low abundance in all other samples. Consistent with the amplicon sequence data, the abundance of 16S rRNA gene copies of Actinobacteria (e.g., Kocuria), and Firmicutes (e.g., Staphylococcus, Virgibacillus) increased after 56 days of culture growth in both ingested and environmental samples (Additional file 1: Figure S4).

Among the bacteria found in the internal mite community, Staphylococcus (OTU_3) did not show a significant relationship either with mite density (GAMM-b, $\chi21 = 0.8$, $P = 0.38$) or guanine (GAMM-b, $\chi21 = 0.1$, $P = 0.80$). Kocuria (OTU_1) showed a significant negative relationship with guanine (GAMM-b, $\chi21 = 4.8$, $P = 0.03$, Fig. 6A) and a positive relationship with mite density (GAMM-b, $\chi21 = 4.7$, $P = 0.03$, Fig. 6B). A different Kocuria sp. (OTU_69) did not show a significant relationship either with mite density (GAMM-b, $\chi^2_1 = 2.3$, $P = 0.13$) or guanine (GAMM-b, $\chi^2_1 = 2.1$, $P = 0.15$). V. pantothenticus (OTU_4) showed a significantly negative relationship with mite density (GAMM-b, $\chi^2_1 = 4.9$, $P = 0.025$, Fig. 5G) and no relationship with guanine (GAMM-b, $\chi^2_1 = 1.8$, $P = 0.19$).

In the environmental samples, V. pantothenticus (OTU_4) did not show a significant relationship either with mite density (GAMM-b, $\chi^2_1 = 0.8$, $P = 0.39$) or guanine (GAMM-b, $\chi^2_1 = 1.0$, $P = 0.32$). L. fermentum (OTU_6) showed a significant negative relationship with guanine (GAMM-b, $\chi^2_1 = 14.7$, $P = 0.0001$, Fig. 6H), but no relationship with mite density (GAMM-b, $\chi^2_1 < 0.1$, $P = 0.88$). O. arenosus (OTU_8) showed significant negative relationship with mite density (GAMM-b, $\chi^2_1 = 219.0$, $P < 0.0001$, Fig. 6C) but no relationship to guanine (GAMM-b, $\chi^2_1 = 0.6$, $P = 0.46$). L. massiliensis (OTU_9) demonstrated significant

negative relationship to both mite density (GAMM-b, $\chi^2_1 = 4.2$, P = 0.04, Fig. 6D) and guanine (GAMM-b, $\chi^2_1 = 13.4$, P = 0.0002, Fig. 6E). Corynebacterium (OTU_4) did not show a significant relationship with either mite density (GAMM-b, $\chi^2_1 < 0.1$, P = 0.95) or guanine (GAMM-b, $\chi^2_1 < 0.1$, P = 0.95). Bacillus (OTU_218) showed a significant negative relationship with mite density (GAMM-b, $\chi^2_1 = 7.0$, P = 0.008, Fig. 6F), but no relationship with guanine (GAMM-b, $\chi^2_1 < 0.1$, P = 0.87).

Fungal microbiome

Alpha diversity metrics were calculated for internal mite fungal communities and the external house dust mite rearing diet (HDMd) fungal community at the level of OTUs. The vast majority of the fungal diversity in both sample types was composed of 3 OTUs (Fig. 2CD), including S. cerevisiae (FOTU_4), Aspergillus penicillioides (FOTU_1), and Candida mucifera (FOTU_3). The commensal and opportunistic pathogenic fungus Malassezia restricta (FOTU_9; e.g., Morand et al. [25]) was detected at a low level in 25 of 90 samples tested. The relative abundance of M. restricta ranged from 0.04–3.94% in the 25 samples tested (mostly in days 14–56, with a median value of 0.16%.

The alpha diversity (Simpson index) of the mite internal fungal community declined significantly over time (GAMM, F1.4 = 7.9, P = 0.005, Fig. 5C), with the community at the final time point (day 84) composed almost entirely of C. mucifera (FOTU_3 and A. penicillioides (FOTU_1). The diversity of external fungal community had a significant increase according to sigmoid function with time (GAMM, F5.7 = 49.5, P < 0.0001, Fig. 5D).

The internal mite fungal community was initially dominated by A. penicillioides (FOTU_1) and C. mucifera (FOTU_3). From days 14–56, S. cerevisiae (FOTU_4) were detected in all internal mite samples and were highly abundant in animals from several flasks. After 56 days, S. cerevisiae were essentially below detection, and the community was again dominated by FOTU_3 C. mucifera and FOTU_1 A. penicillioides, though the relative abundance of these taxa varied by time point. In the HDMd samples, the fungal community was strongly influenced by the presence of the yeast S. cerevisiae (FOTU_4) at the beginning of mite culture growth, as yeast was a component of the diet (Additional file 1: Figures S4). The relative abundance of S. cerevisiae (FOTU_4) gradually decreased during mite culture growth and was replaced by A. penicillioides (FOTU_1) and C. mucifera (FOTU_3; Fig. 2CD). This result was confirmed by qPCR with specific primers (Additional file 1: Figure S5). No significant relationship between the abundance of S. cerevisiae and mite density (GAMM-b, $\chi^2_1 = 1.8$, P = 0.18) or guanine (GAMM-b, $\chi^2_1 = 0.2$, P = 0.68) was observed.

In the environmental samples (HDMd), A. penicillioides (FOTU_1) showed a significant positive relationship with guanine (GAMM-b, $\chi^2_1 = 22.1$, P < 0.0001, Fig. 6A) and no relationship to mite density (GAMM-b, $\chi^2_1 = 1.5$, P = 0.22). C. mucifera (FOTU_3) also showed a significantly positive relationship with guanine (GAMM-b, $\chi^2_1 = 6.7$, P = 0.01, Fig. 6B) and no relationship to mite density (GAMM-b, $\chi^2_1 = 1.5$, P = 0.22). S. cerevisiae (FOTU_4) showed a significantly negative relationship with guanine (GAMM-b, $\chi^2_1 =$

6.3, P = 0.01, Fig. 7C) and no relationship to mite density (GAMM-b, $\chi^2_1 < 0.1$, P = 0.97). C. mucifera (FOTU_413) did not show a significant relationship either with mite density (GAMM-b, $\chi^2_1 < 0.1$, P = 0.95) or guanine (GAMM-b, $\chi^2_1 = 3.2$, P = 0.07). Xerochrysium xerophilum (FOTU_412) did not show a significant relationship either with mite density (GAMM-b, $\chi^2_1 < 0.1$, P = 0.98) or guanine (GAMM-b, $\chi^2_1 = 1.9$, P = 0.17). C. mucifera (FOTU_521) did not show a significant relationship either with mite density (GAMM-b, $\chi^2_1 < 0.1$, P = 0.81) or guanine (GAMM-b, $\chi^2_1 < 0.1$, P = 0.82).

Discussion

In this study, we hypothesized that the concentration of mite nitrogenous waste products and mite population density influence microbial community structure inside mites and in the environmental culture of D. pteronyssinus. We previously observed differences in the microbiome composition of mites from young and old cultures [14] and the time changes of microbiome during colony culture growth of D. farinae [26]. Thus, we expected that the mites contaminate their environment by through their nitrogenous waste product guanine [18–20], which can serve as nutrient source for microorganisms. In contrast, increasing mite density increases the mite grazing effect on some microorganisms due to the selective feeding [27, 28]. In our experiments, the composition of mite microbial communities was remarkably consistent between replicates and composed of relatively few dominant taxa – 11 bacterial OTU and 3 fungal OTU. By plating of D. pteronyssinus cultures, we also identified bacterial taxa that were not detected by barcode sequencing in this study (i.e., Micrococcus aloeverae and Paenibacillus glucanolyticus) and fungal taxa (i.e., Penicillium griseofulvum, Penicillium brasilianum, and Hyphopichia pseudoburtonii) [29] which are the result of different methodical approach (e.g., PCR bias and depth of sequencing can contribute to distinct observed microbial communities in cultivation-dependent and cultivation-independent methods). The external bulk microbiome (i.e., the bulk medium containing food and mite excretions) presented a unidirectional shift in the structure of both bacterial and fungal communities, with increasing diversity over time, with the exception of fungal diversity in the mite internal culture, which showed a slight decrease. The microbial taxa observed in the environmental samples at the start of the experiment were nearly exclusively L. fermentum and S. cerevisiae, and these taxa were almost entirely absent by the end of the experiment.

The study confirmed the above described pattern of culture growth in D. pteronyssinus; however, we identified different durations of culture growth phases [5, 16, 17]. We were not able to distinguish the latency phase because our cultures were started with a high number of mites from the beginning; this also resulted in faster culture cycle, i.e. decline after 84 days. Similarly, shortening of the culture time and absence of latency phase was observed for D. farinae previously [26]. During culturing, the mites produce guanine, a nitrogenous waste metabolite [18–20]. The dynamic of concentration and microcosm respiration showed similar patterns to D. farinae [26]. The nitrogenous waste dynamics is connected to the density of mite population, decreasing in the decline phase of D. pteronyssinus for D. farinae [26]. The microbial respiration in microcosms showed two small peaks after 30 and 70 days in the both species of mites [26]. However, the two peaks of respiration detected here were not related to the microbial biomass

evaluated here as the numbers of DNA copies amplified by universal primers. Previously we discussed the relationship between decreases of respiration and explained the first decrease of respiration by the decrease of S. cerevisiae and the second one connected to the decrease microbial biomass expressed as the numbers of copies of 18S rDNA in the samples of culture in the decline phase [26]. One explanation is that there were exchanges in the microbial community after both peaks of respiration. However, we did not find any effect of respiration on the composition of microbial community.

Culture growth time was the most important factor influencing the composition of microbes. This result agrees well with our previous findings for house dust mite cultures [14, 26]. The general explanation for saprophagous arthropods is that the arthropods influence the microorganisms by vectoring of microorganisms, selective feeding, opening the free spaces to microbial growth by diet fragmentation and waste production which modifies the culture environment [30]. The effect of these mite activities are suggested to increase with increasing mite population density [31]. In this study, mite population density increased during culture growth up until the decline phase. Although we did not measure vectoring and feeding directly, these are connected to mite density.

The ability of mites to change their culture environment through feeding activity and feces production was reported for stored product mites T. putrescentiae and fungal cultures [32, 33]. Feeding on fungi was well documented for D. pteronyssinus [34, 35]. The selective feeding of D. pteronyssynus on S. cerevisiae was expected, and earlier experiments have shown that the addition of yeasts to wheat germ flakes accelerated the growth of mites, though the population density was lower than on dried fish meal [36]. Mite feeding and digestion of S. cerevisiae explains the decrease of the numbers of yeasts in the culture; and rapid digestion can reduce the number of yeast DNA copies in the mite gut. We hypothesize that mite feeding on the yeasts leads to overgrazing and replacement by A. penicillioides. A previous study showed that this fungus was introduced to the culture via mites [37]. The microbiome analyses in the current study supports this finding, because the mites introduced into the culture contained 50% of A. penicillioides reads. The density of the fungus (observed as the numbers of its spores) increased in the culture with increasing time and mite density [37]. Here we detected a positive relationship between guanine and the relative abundance of amplicons derived from A. penicillioides in the environmental culture, and this may indicate that this fungus uses guanine as a source of nitrogen for mycelial growth. In prior studies, mites were able to feed on this fungus, but their fitness decreased in terms of survival which led to reduced population growth [38]. However, the mites were not able to produce second generation on an axenic diet without A. penicillioides fungus [38]. In this study, the relative abundance of C. mucifera increased with culture time in both inside mite and environmental culture samples. Prior studies have shown that the addition of a similar taxon Trichomonascus ciferrii (Candida ciferrii) to the diets of mites accelerates population growth of D. pteronyssinus in comparison to the rearing diet [29]. This demonstrates that both A. penicillioides and C. mucifera can serve as a food source for mites in the later stages of mite culture growth.

Similar to the previous findings for the D. farinae microbiome [14], no known acaropathogenic bacteria were identified here. This finding is consistent with the known microbiome of Korean strains of house

dust mites [7, 13]. In general, bacteria have been suggested to be of lower importance than fungi for D. pteronyssinus population growth in comparison to the role in the growth of D. farinae [39]. This was observed in a study in which Micrococcus lysodeikticus was added to the mite diet, and the acceleration of D. farinae population growth in the comparison to control diet was measured [39]. However, in more recent laboratory experiments, addition of Bacillus cereus, Micrococcus aloeverae and Kocuria rhizophila into the diet decreased population growth rate of D. pteronyssinus mites in comparison to control diet, while addition of Staphylococcus nepalensis and Paenibacillus glucanolyticus, in turn, increased mite population growth rate [29]. In another study, a B. cereus strain isolated from T. putrescentiae feces was added to two types of diets, leading to decreased T. putrescentiae growth. The effect was much higher when the basis of the mite diet was dry dog food (rich in protein and fat) as compared to whole-meal spelt flour [40]. Thus, the diet used does affect bacterial growth, and although bacterial communities appear to be strongly associated with mites (mutualistic), some biotests indicated suppressive action by some bacterial taxa [40]. Mite-microbe-diet interactions are complex, and microorganisms can serve as commensals, antagonists, and as food. In addition, the type of diet can influence the mite environmental community composition. Mite bodies and feces could serve as microbial vectors and/or their reservoirs in mite cultures much in the same way as they do for fungi. Furthermore, some bacteria such as B. cereus can grow on mite bodies, exuviae and feces, providing a highly interactive relationship [40]. Similarly, the data presented in this study suggest that bacteria from the genera Kocuria, Virgibacillus, and Staphylococcus are introduced to the bulk culture media from the mites themselves, and this introduction is visible by 14 days of cultivation. Staphyloccus and Kocuria belong to the most frequently identified bacteria from the isolates obtained by plating D. farinae mites [41]. Thus, these bacteria appear to be carried by D. pteronyssinus from environment to environment through mite bodies and feces. Mites can change their feeding preference to consume diets with more Staphyloccocus, which could increase in the mite internal profiles of 40- and 84-day old samples. Guanine concentration in the bulk medium can inhibit growth of the bacteria; we observed a negative correlation between guanine and the bacterial taxa L. fermentum, L. massiliensis, and O. arenosus. However, these data are based on sequencing results and therefore represent relative abundance. Thus, in relative numbers, a shift in absolute abundance that is masked by changes in the proportions of other taxa in a sample.

It has been suggested that feeding of mites on A. penicillioides does not contribute to the allergenicity of D. pteronyssinus [38]. The allergen profiles of experimentally-derived fungus-free and fungus-fed mites were shown to be identical [38]. Thus, it is likely that there are other factors that influence allergen production besides the fungi. Other studies have shown that there are differences in allergen profiles among extracts from exponentially growing and declining mite cultures [5, 16, 17]. These differences could be associated to the population demographic parameters (juveniles/adult proportion) and/or by adaptation to the diet. Standard mite diets include S. cerevisiae, but the addition of other components, including proteins, lipids, and carbohydrates, modulates the major allergens Der p 1 or Der p 2 content in the mite bodies [42]. Although previous observation did not confirm the effect A. penicillioides on allergen production, the feeding of mites on other microorganisms can modulate the production, because they contains different nutrients than standardized diets.

We did not detect any Gram-negative bacteria that increased in relative abundance during growth of the mite D. pteronyssinus in this study. The data observed here indicate that our mite cultures contain almost no reads of Gram-negative bacteria, e.g., Bartonella-like bacteria [6] and Gram-negative parasitic Cardinium [43] observed in D. farinae. The observed absence of Gram-negative bacteria is important from a medical perspective because Gram-negative bacteria can produce endotoxins (i.e., heat stable lipopolysaccharides), contaminating commercially produced allergen extracts [6, 7]. However, we cannot exclude the possibility that Gram-negative bacteria could contaminate cultures under certain circumstances and become problematic. To confirm these findings more strains of D. pteronyssinus should be studied, and highly sensitive quantitative PCR assays can be employed to target bacterial taxa of interest.

One important finding of our study is the presence of Malassezia in the ingested community, although at low relative abundance (e.g. median values of 0.16%). Based on the proportion of the reads and the presence of the taxon in D. farinae [26], we believe that it is not a contaminant or other artifact of this study. Malassezia yeasts represent lipid-dependent and lipophilic organisms that are part of the skin microflora, but can be involved in skin disorders such as dermatitis or otitis eczema in humans and pet animals [44–46]. Our rearing diet did not contain any human or animal skin (a food source for Malassezia), and one possible explanation is that the Malassezia yeast detected in this study are part of a long-term symbiotic association with the mite D. pteronyssinus. We therefore propose the following hypotheses: (i) mites can be reservoirs and vectors of these yeasts, and (ii) in sensitive individuals, mite allergens can interact with the yeast in the development of cutaneous allergy diseases. Future research, including nutritional-based studies and better identification of Malassezia strains, will be necessary to confirm these hypotheses.

Conclusion

In this study we show that the microbiome in cultures of the European house dust mite D. pteronyssinus, although composed of relatively few dominant taxa, is dynamic during culture growth. The microbial community structure of the bulk culture environment shows a unidirectional progression over time, while the internal mite microbial community structure oscillates. Profile changes in microbiomes may be explained by the effects of mite population density and guanine, which accumulates during mite growth. In the mite microbiome, we detected Malassezia yeast (human and animal opportunistic pathogen. In our study, no increase in the relative abundance of potential endotoxin producing Gram-negative bacteria was observed as the bacterial community was dominated by Gram-positive bacteria.

Materials And Methods

Mites

The European house dust mite (Dermatophagoides pteronyssinus) culture was obtained from the allergen/vaccine producing company at Trebon, Czechia (RNDr. Alexandr Zgarbovsky) in 2005. The

culture was maintained under laboratory conditions in darkness with controlled humidity (75% RH) and temperature (25 ± 1 °C). The mites were reared in tissue culture flasks with a 25-cm^2 surface and 70-mL capacity (Iwaki flasks; cat. no. 3100-025; Sterilin, Newport, United Kingdom). The flasks were maintained in a Secador desiccator (Bel-Art Products, Pequannock, NJ, USA) with a saturated NaCl solution. The diet (HDMd) consisted of a mixture of dog food/wheat germ/dried fish food/Pangamin dried yeast (S. cerevisiae) extract/gelatin at a ratio of 10/10/3/2/1 w/w. All the compounds were mill-powdered, sieved (mesh size 500 µm) and pasteurized by heating to 70 °C for 0.5 h [39]. The colonies were sub-cultured monthly in the rearing facility. To establish a new culture, approximately 5,000 mites were placed in a new chamber containing 0.3 g of freshly prepared diet.

Experimental design

Our experimental design is detailed in Additional file 1: Figure S4. Experiments were conducted in six replicates, in six 660-mL capacity flasks (Cellstar®, Greiner Bio-One, Frickenhausen, Germany, cat. no. 660 – 150) with 36 g of HDMd. Mites were transferred into each experimental flask from the six rearing flasks containing 30-day-old mite cultures. Every rearing flask contained approximately 0.3 g of rearing medium and approximately 5,000 mites. The culture populations were then sampled at 14, 28, 42, 56, 70, 84, and 98 days. Each sample included all mite developmental stages in six replicates. The rearing diet without mites (SPGM) was sampled by the same method in six replicates.

Sampling design

Live mites and SPGM (spent culture medium) were sampled from the same culture chambers at different periods of culture development under aseptic conditions (Table 1). For DNA extraction, live mites were collected from the chamber plug with a brush, then the mite samples (Additional file 2: Table S2) were weighed on a microbalance and transferred to a 1.5 mL Eppendorf tube filled with 100% ethanol. After collecting of live mites, the chamber was shaken gently to obtain a homogenous mix of the diet and mites. The mixture of diet + mites was sampled, the diet + mites were weighed and used to different tasks: (i) respiration measurement; (ii) mite density estimation, (iii) DNA extraction from diets after mite removal (SPGM - mite culture debris: rest of diets, feces, no mites or eggs), (iv) guanine contents measurement; (v) mite histology.

Table 1
Multivariate analysis of variance by permutation (PEMANOVA). Significant differences are indicated by bold.

Microbiome	**Bacteria**							
	Internal mite				**Environmental culture**			
	Df	**R2**	**F**	**P**	**Df**	**R2**	**F**	**P**
Time	1	0.121	4.967	< 0.001	1	0.313	23.019	< 0.001
Population density	1	0.049	2.022	0.057	1	0.196	14.388	< 0.001
Microcosm respiration	1	0.040	1.642	0.104	1	0.019	1.376	0.204
Guanine contents	1	0.034	1.402	0.163	1	0.054	3.963	0.003
Time : Pop. density	1	0.040	1.659	0.101	1	0.013	0.920	0.431
Time : Respiration	1	0.017	0.719	0.663	1	0.015	1.071	0.345
Time :Guanine	1	0.017	0.681	0.712	1	0.012	0.857	0.480
Residual	28	0.681			28	0.380		
Total	35	1.000			35	1.000		
Microbiome	Fungi							
	Internal mite				Environmental culture			
	Df	R2	F	P	Df	R2	F	P
Time	1	0.085	3.687	0.001	1	0.598	59.496	< 0.001
Population density	1	0.135	5.875	< 0.001	1	0.034	3.356	0.041
Microcosm respiration	1	0.020	0.869	0.511	1	0.010	1.029	0.322
Guanine contents	1	0.021	0.918	0.458	1	0.018	1.751	0.157
Time : Pop. density	1	0.053	2.287	0.020	1	0.039	3.860	0.028
Time : Respiration	1	0.014	0.621	0.867	1	0.010	1.028	0.326
Time : Guanine	1	0.026	1.118	0.288	1	0.010	1.032	0.315
Residual	28	0.646			28	0.281		
Total	35	1.000			35	1.000		

Legend: Environmental culture spent growth medium (SPGM - extracts from the mite culture medium and feces without mites); internal mite - the bacteria from the samples of surface sterilized mites; Time – sampling time.

Density estimate

Mites and diet were weighed and transferred to 1.5 mL Eppendorf tubes filled with 80% ethanol. Then, the mites were counted under a dissecting microscope. The number of mites was recalculated for each sample per 0.01 g of diet. We did not distinguish between adults and juveniles. Following previous studies [17], eggs were not counted.

Respiration measurement

We used a previously described protocol [47]. Respiration was measured using an IRGA gas analyzer and respiration apparatus (catalog no. RP1LP, Qubit Systems, Kingston, ON, Canada) based on a Gas-card II infrared card (Edinburgh Sensors, Scotland, United Kingdom) in syringes containing diet taken from the mite cultures after two hours of incubation at 25 ± 0.1 °C. Carbon dioxide (CO_2) produced in the chamber was measured in µL per mg of diet fresh weight per hour ($\mu L \cdot mg^{-1} \cdot h^{-1}$). Based on previous studies, the respiration of extract from SPGM is mostly linked to the microbial activity, while the mite respiration was marginal [48].

Histology

For microanatomical observations, we used previously described protocols for paraffin histology. The mites were fixed in modified Bouin-Dubosque fluid, embedded in paraffin and sectioned [49]. We focused on the analyses of gut contents and the status of mites in the declining culture.

Guanine measurement

SPGM samples from the rearing chambers were lyophilized in 15-mL centrifuge tubes covered with filters in a PowerDry LL3000 (Thermo; Waltham, MA, USA), and 0.1 g of the sample was homogenized in 3 mL of ammonium acetate buffer (pH = 3.5) using 0.1 g of an equal mixture of garnet sharp particles (0.3/1.0 mm diameter particles; BioSpec, Bartlesville, OK, USA; cat. no. 11079103 and 11079110) and vortexed. Then, the sample was treated in an ultrasonic bath for 30 min (30 °C). After this treatment, 0.12 g of sorbent mixture (1:1 C_{18} ec and Diamino sorbents, Macherey-Nagel, Duren, Germany) was added to the sample and mixed by vortexing. The samples were centrifuged for 10 min at 10,232 g. Then, 1 mL of each sample was filtered through regenerated cellulose syringe filters of 0.45 µm pore size (TR-200435; diameter 13 mm, Teknokroma, Barcelona, Spain) into a 2 mL glass vial. The analysis was conducted using an Agilent high-performance liquid chromatography system (1200 series; Agilent Technologies Deutschland, Waldbronn, Germany) equipped with a degasser, quaternary pump, autosampler, thermostat and diode-array detector. The chromatographic separation was performed on a Kinetex C18 analytical column (150 mm × 4.6 mm, 2.6 µm; Phenomenex, Torrance, CA, USA) protected by a guard column with C18 cartridge (4 mm × 3.0 mm; Phenomenex). The column temperature was maintained at 24 °C throughout the analysis. Separation was performed with a flow rate of 0.5 mL/min using an injection volume of 5 µL and the following gradient: (A) 20 mM ammonium acetate buffer (3.5 pH) and (B) methanol; 0.0 min, 100% A; 10–11 min, 80% A; 17 min, 100% A. The instrument control and data evaluation were performed using OpenLab software (Agilent). The calibration and extraction

efficiency were evaluated with guanine (cat. no. G6779 Sigma-Aldrich). Non-matrix-matching quantification was performed (samples always contain guanine). The final concentration of guanine was expressed in mg/g.

DNA extraction

Mite samples were surface cleaned by removing the 100% ethanol after centrifugation (13,000 x g for 1 min) and replacing it with bleach, vortexing for 5 s and removing the bleach after centrifugation (13,000 x g for 1 min). Then, the samples were washed in 100% ethanol twice to remove the rest of the bleach using centrifugation. DNA was extracted using the Exgene™ Genomic DNA micro kit (Cambio, Cambridge, UK, cat. no. GA-118-050) with 300 µL CL buffer (kit component) replacing the ethanol, and the solution was removed under a sterile hood. The mites were transferred to a 2.0 ml Screwcap MCT conical NS (cat. no. CP5912, Alpha Laboratories, Eastleigh, Hampshire, UK) with 0.5 g of an equal mixture of 0.3 mm and 1.0 mm garnet sharp particles (cat. nos. 11079103gar and 11079110gar, BioSpec) and 1 glass bead (3 mm diameter, cat. no. R155761, BioSpec). The samples were homogenized in a Mini-BeadBeater (BioSpec) for 5 min. The homogenates were centrifuged (10,000 x g for 2 min), the supernatant was transferred to a new sterile Eppendorf tube, and 20 µL of proteinase K was added. The sample was incubated at 56 °C overnight. The rest of the isolation was performed according to the manufacturer's instructions.

SPGM from the experimental flask was mixed with 50 mL of sterile phosphate buffered saline (PBST – 3.2 mM Na_2HPO_4, 0.5 mM KH_2PO_4, 1.3 mM KCl, and 135 mM NaCl) with 0.05% w/w Tween® 20 detergent (Sigma-Aldrich) [41] and vortexed for 5 s. The mixture was filtered through a 40 µm mesh Cell Strainer (cat. no. 27305, Stemcell Technologies, Cambridge, MA, USA) to remove the remaining diet and any mite bodies. The filtered supernatant was centrifuged (845 x g, 5 min), the supernatant was discarded, and the pellets were cleaned by washing in PBST and centrifugation. The clean pellets were finally resuspended in 10 mL of PBST and frozen (-40 °C). DNA extraction was performed by transferring 1 mL of the supernatant to a 1.5 mL Eppendorf tube and using the Exgene™ Genomic DNA micro kit. The tubes were centrifuged (6,785 x g; 3 min), the supernatant was discarded, and the pellets were suspended in 200 µL of CL buffer. Then, 20 µL of proteinase K was added, and the samples were incubated at 56 °C overnight. The rest of the procedure was performed according to the manufacturer's instructions. The isolated DNA was stored at -20 °C until analysis. The quality of the isolated DNA was established by running PCR with universal primers and using a NanoDrop One (Thermo-Fisher Scientific, Waltham, MA, USA) (Additional file 1: Table S1).

Barcode sequencing

Portions of the18S rRNA gene were used for characterization of the fungal microbial community. DNA was amplified using the CS1_FF390 and CS2_FR1 primers (Additional file 1: Table S1) and a previously described amplification protocol, i.e., PCR amplification started at 95 °C for 8 minutes, followed by 28 cycles with 95 °C – 30 s, 50 °C – for 45 s, 68 °C -120 s and ended at 72 °C for 10 minutes. [50–52]. For bacterial barcoding the V4 variable region of the microbial 16S rRNA gene was used. As chloroplast DNA

can influence the profiling of arthropod bacterial communities [53], we used a protocol that prevents chloroplast DNA from amplifying [54]. Initially, samples were amplified with the primers F27 and an equimolar mixture of the 783r-aL, 783r-bL and 783r-cL modified reverse primers (Additional file 1: Table S1) [54] to reduce the impact of chloroplast DNA amplification. Subsequently, these PCR amplicons were amplified with the CS1_515F and CS2_806R primers (Additional file 1: Table S1) [51, 55]. We added 1 μL of the reaction product to the next PCR reaction. Takara Ex Taq DNA polymerase and master mix (cat. no. RR001A, Takara Bio, Saint-German-en-Laye, France) were used. The negative control was ddH2O. Amplicons were sequenced at the University of Illinois at Chicago Sequencing Core (UICSQC), on a MiSeq platform (Illumina, San Diego, CA, USA) [56]. The sequences (2 × 153–16S or 2 × 250–18S) were demultiplexed and the barcodes and primers were removed by the company. Raw sequences of the 16S rRNA gene and 18S rRNA gene amplicons were submitted to the Sequence Read Archive (SRA) with the accession number SRP150479 (Additional file 1: Table S1). The forward and reverse sequences were merged and processed using a combination of MOTHUR 1.40.0 [57] and UPARSE 10 [58, 59] according to the standard procedures [60]; mismatches/ambiguous sequences, chimeras, chloroplast and mitochondria sequences were removed during the process. Sequence data were clustered into OTUs at a level of 97% of similarity. The OTUs were annotated using the Ribosomal Database Project [61], with training set No. 15 for bacteria and Silva128 for fungi [62]. Representative sequences for each OTU were then compared to those in GenBank using BLASTn [63] (Additional file 2: Tables S2 and 3). The names for OTUs are based on the highest similarity to the sequences in GenBank. In the bacterial dataset, all OTUs with fewer than 1000 total reads were removed from further analyses. Both datasets were rarefied to a depth of 5000 sequences/sample (Additional file 2: Tables S4 and S5).

qPCR

A previously described protocol [14, 64] was applied; primers and PCR profiles are detailed in Additional file 1: Table S1. Fragments of the 16S and 18S rRNA genes were used as standards. DNA used in the qPCR analyses originated from the same samples used for the barcode sequencing to identify the quantity of the selected microbial groups. The analyses included two technical replicates, which were then averaged. The DNA copy numbers were recalculated for each mite or extract sample. The data were log(10)-transformed before analysis. Specific primers targeting 16S rRNA genes of Wolbachia, Cardinium and S. cerevisiae provided low numbers of copies (0–27 copies per mite) in the mite body samples. We exclude them from the analyses and indicated them below detection (Additional file 2: Table S9).

Data analyses

PAST [65] and R software [66] were applied with the vegan [67], adespatial [68] and mgcv [69] packages. Temporal changes in the population size, amount of guanine, and respiration were modelled by means of Generalized Additive Mixed Models (GAMM) because most responses were strongly nonlinear, not normally distributed and included temporal replications arising from repeated measurements. As a result, mite rearing chamber was a random effect in each model. When modelling the mite population density, the logarithm of mass of culture was used as an offset. The linear predictor included thin-plate spline function for time. The population size and respiration were assumed to have gamma errors (GAMM-g),

guanine content and Simpson index of diversity to have normal errors (GAMM). The proportion of reads of selected bacteria and fungi was modelled to the mite density and amount of guanine while controlling for the time by means of GAMM with beta errors (GAMM-b). For beta diversity analyses, the barcode sequencing data were analyzed via Bray–Curtis dissimilarity. The means per rearing chamber or medians per sampled time were used to observe the effect of population density and SPGM respiration on microbial profiles in the D. pteronyssinus microbiome; these statistics were then analyzed with non-parametric PERMANOVA [70] using the adoins2 function in R (100,000 permutations). Non-metric multidimensional scaling (NMDS) was applied for visualization of PERMANOVA results. Robustness of clustering was demonstrated using boot-strap analysis (1000 iterations). Heatmaps were constructed for log2 transformed data of standardized reads in XL STAT (https://www.xlstat.com/en). The differences among sampling time for separate OTUs were calculated using METASTATS in Mothur using 10,000 bootstrap iterations.

Declarations

Acknowledgements

We thank Marie Bostlova, Martin Markovic, and Jan Hubert Jr. for technical assistance. We are grateful to Alexandr Zgarbovsky for *Dermatophagoide*s mites. The authors are grateful to the anonymous referees for their valuable comments.

Authors' contribution

JH, VM, and MN designed the study, mite culture rearing MN, molecular biology SJG, MN, biotests MN and VM, guanine contents analyses ES, bioinformatical analyses and statistic JH, statistical analyses SP, scientific writing JH, SP, SJG, PBK, ES, VM, TE.

Funding

JH, TE, ES, VM, and MN were supported by the Czech Science Foundation (GACR) as part of Project No. 17-12068S and by the project Ministry of Agriculture RO418. PBK was supported by the Russian Science Foundation, Project No. 19-14-00004.

Availability of data and materials

Sequence data have been deposited in the GenBank Short Read Archive (SRA) under the BioProject ID number PRJNA534281 (Additional file 1: Table S1). The datasets are included in supplementary tables (Additional file 2: Tables S4–S9).

Ethics approval and consent

Not applicable.

Conflict of interest

The authors declare no conflict of interest.

ORCID

Marta Nesvorna https://orcid.org/0000-0003-0572-4131

Vit Molva https://orcid.org/0000-0002-4504-5355

Stano Pekar https://orcid.org/0000-0002-0197-5040

Elena Shcherbachenko https://orcid.org/0000-0002-1312-389X

Tomas Erban https://orcid.org/0000-0003-1730-779X

Stefan J. Green https://orcid.org/0000-0003-2781-359X

Pavel B. Klimov https://orcid.org/0000-0002-9966-969X

Jan Hubert https://orcid.org/0000-0003-0740-166X

References

1. Colloff MJ. Dust mites. Collingwood, VIC: CSIRO Publishing; 2009.
2. WHO/IUIS. Allergen Nomenclature: Allergen TreeView. WHO/IUIS Allergen Nomenclature Sub-Committee. 2019. http://allergen.org/treeview.php. Accessed 10 May 2019.
3. Tang VH, Stewart GA, Chang BJ. *Dermatophagoides pteronyssinus* lytFM encoding an NlpC/P60 endopeptidase is also present in mite-associated bacteria that express LytFM variants. FEBS Open Bio 2017;7:1267–80.
4. Erban T, Harant K, Hubert J. Detailed two-dimensional gel proteomic mapping of the feces of the house dust mite *Dermatophagoides pteronyssinus* and comparison with *D. farinae*: reduced trypsin protease content in *D. pteronyssinus* and different isoforms. J Proteomics 2017;162:11–9.
5. Eraso E, Martinez J, Martinez A, Palacios R, Guisantes JA. Quality parameters for the production of mite extracts. Allergol Immunopathol. 1997;25:113–7.
6. Valerio CR, Murray P, Arlian LG, Slater JE. Bacterial 16S ribosomal DNA in house dust mite cultures. J Allergy Clin Immunol. 2005;116:1296–300.
7. Lee J, Kim JY, Yi M-h, Hwang Y, Lee I-Y, Nam S-H, et al. Comparative microbiome analysis of *Dermatophagoides farinae*, *Dermatophagoides pteronyssinus*, and *Tyrophagus putrescentiae*. J Allergy Clin Immunol. 2019;143:1620–3.
8. Jacquet A. The role of the house dust mite-induced innate immunity in development of allergic response. Int Arch Allergy Immunol. 2011;155:95–105.
9. Gregory LG, Lloyd CM. Orchestrating house dust mite-associated allergy in the lung. Trends Immunol. 2011;32:402–11.

10. Hubert J, Nesvorna M, Klimov P, Dowd SE, Sopko B, Erban T. Differential allergen expression in three *Tyrophagus putrescentiae* strains inhabited by distinct microbiome. Allergy 2019;74:2502–7.
11. Hubert J, Kopecky J, Sagova-Mareckova M, Nesvorna M, Zurek L, Erban T. Assessment of bacterial communities in thirteen species of laboratory-cultured domestic mites (Acari: Acaridida). J Econ Entomol. 2016;109:1887–96.
12. Molva V, Bostlova M, Nesvorna M, Hubert J. Do the microorganisms from laboratory culture spent growth medium affect house dust mite fitness and microbiome composition? Insect Sci. 2020;27:266–75.
13. Kim J-Y, Yi M-H, Hwang Y, Lee JY, Lee I-Y, Yong D, et al. 16S rRNA profiling of the *Dermatophagoides farinae* core microbiome: *Enterococcus* and *Bartonella*. Clin Exp Allergy 2018;48:607–10.
14. Hubert J, Nesvorna M, Kopecky J, Erban T, Klimov P. Population and culture age influence the microbiome profiles of house dust mites. Microb Ecol. 2019;77:1048–66.
15. Eraso E, Guisantes JA, Martinez J, Saenz-de-Santamaria M, Martinez A, Palacios R, et al. Kinetics of allergen expression in cultures of house dust mites, *Dermatophagoides pteronyssinus* and *D. farinae* (Acari: Pyroglyphidae). J Med Entomol. 1997;34:684–9.
16. Martinez J, Eraso E, Palacios R, Guisantes JA. Enzymatic analyses of house dust mite extracts from *Dermatophagoides pteronyssinus* and *Dermatophagoides farinae* (Acari: Pyroglyphidae) during different phases of culture growth. J Med Entomol. 1999;36:370–5.
17. Eraso E, Martinez J, Garcia-Ortega P, Martinez A, Palacios R, Cisterna R, et al. Influence of mite growth culture phases on the biological standardization of allergenic extracts. J Investig Allergol Clin Immunol. 1998;8:201–6.
18. Levinson HZ, Levinson AR, Muller K. Functional adaptation of two nitrogenous waste products in evoking attraction and aggregation of flour mites (*Acarus siro* L.). Anz Schadlingskde Pflanzenschutz Umweltschutz 1991;64:55–60.
19. Levinson HZ, Levinson AR, Muller K. The adaptive function of ammonia and guanine in the biocoenotic association between ascomycetes and flour mites (*Acarus siro* L.). Naturwissenschaften 1991;78:174–6.
20. Levinson HZ, Levinson AR, Offenberger M. Effect of dietary antagonists and corresponding nutrients on growth and reproduction of the flour mite (*Acarus siro* L.). Experientia 1992;48:721–729.
21. van Bronswijk JEMH. Guanine as a hygienic index for allergologically relevant mite infestations in mattress dust. Exp Appl Acarol. 1986;2:231–8.
22. van Bronswijk JEMH, Bischoff E, Schirmacher W, Kniest FM. Evaluating mite (Acari) allergenicity of house dust by guanine quantification. J Med Entomol. 1989;26:55–9.
23. Hanlon RDG. Influence of grazing by Collembola on the activity of senescent fungal colonies grown on media of different nutrient concentration. Oikos 1981;36:362–7.
24. Siepel H, Maaskamp F. Mites of different feeding guilds affect decomposition of organic matter. Soil Biol Biochem. 1994;26:1389–94.

25. Morand SC, Bertignac M, Iltis A, Kolder ICRM, Pirovano W, Jourdain R, et al. Complete genome sequence of *Malassezia restricta* CBS 7877, an opportunist pathogen involved in dandruff and seborrheic dermatitis. Microbiol Resour Announc. 2019;8:e01543-18.
26. Klimov P, Molva V, Nesvorna M, Pekar S, Shcherbachenko E, Erban T, et al. Dynamics of the microbial community during growth of the house dust mite *Dermatophagoides farinae* in culture. FEMS Microbiol Ecol. 2019;95:fiz153.
27. Van Asselt L. Interactions between domestic mites and fungi. Indoor Built Environ. 1999;8:216–20.
28. Hubert J, Jarosik V, Mourek J, Kubatova A, Zdarkova E. Astigmatid mite growth and fungi preference (Acari: Acaridida): comparisons in laboratory experiments. Pedobiologia 2004;48:205–14.
29. Molva V, Nesvorna M, Hubert J. Feeding interactions between microorganisms and the house dust mites *Dermatophagoides pteronyssinus* and *Dermatophagoides farinae* (Astigmata: Pyroglyphidae). J Med Entomol. 2019;56:1669–77.
30. Nalepa CA, Bignell DE, Bandi C. Detritivory, coprophagy, and the evolution of digestive mutualisms in Dictyoptera. Insect Soc. 2001;48:194–201.
31. Crowther TW, Boddy L, Jones TH. Functional and ecological consequences of saprotrophic fungus–grazer interactions. ISME J. 2012;6:1992–2001.
32. Smrz J, Catska V. The effect of the consumption of some soil fungi on the internal microanatomy of the mite *Tyrophagus putrescentiae* (Schrank) (Acari, Acaridida). Acta Univ Carol Biol. 1989;33:81–93.
33. Smrz J, Svobodova J, Catska V. 1991. Synergetic participation of *Tyrophagus putrescentiae* (Schrank) (Acari; Acaridida) and its associated bacteria on the destruction of some soil micromycetes. J Appl Entomol. 1991;111:206–10.
34. de Saint Georges-Gridelet D. Vitamin requirements of the European house dust mite, *Dermatophagoides pteronyssinus* (Acari: Pyroglyphidae), in relation to its fungal association. J Med Entomol. 1987;24:408–11.
35. Douglas AE, Hart BJ. The significance of the fungus *Aspergillus penicillioides* to the house dust mite *Dermatophagoides pteronyssinus*. Symbiosis 1989;7:105–16.
36. van Bronswijk JEMH. Food preference of pyroglyphid house-dust mites (Acari). Neth J Zool. 1971;22:335–40.
37. Petrova-Nikitina AD, Antropova AB, Bilanenko EN, Mokeeva VL, Chekunova LN, Bulgakova TA, et al. Population dynamics of mites of the family pyroglyphidae and micromycetes in laboratory cultures. Entomol Rev. 2011;91:377–87.
38. Hay DB, Hart BJ, Douglas AE. Effects of the fungus *Aspergillus penicillioides* on the house dust mite *Dermatophagoides pteronyssinus*: an experimental re-evaluation. Med Vet Entomol. 1993;7:271–4.
39. Erban T, Hubert J. Digestive function of lysozyme in synanthropic acaridid mites enables utilization of bacteria as a food source. Exp Appl Acarol. 2008;44:199–212.
40. Erban T, Rybanska D, Harant K, Hortova B, Hubert J. Feces derived allergens of *Tyrophagus putrescentiae* reared on dried dog food and evidence of the strong nutritional interaction between the

mite and *Bacillus cereus* producing protease bacillolysins and exo-chitinases. Front Physiol. 2016;7:53.

41. Hubert J, Kopecky J, Perotti MA, Nesvorna M, Braig HR, Sagova-Mareckova M, *et al*. Detection and identification of species-specific bacteria associated with synanthropic mites. Microb Ecol. 2012;63:919–28.
42. Vidal-Quist JC, Ortego F, Rombauts S, Castanera P, Hernandez-Crespo P. Dietary shifts have consequences for the repertoire of allergens produced by the European house dust mite. Med Vet Entomol. 2017;31:272–80.
43. Erban T, Klimov P, Molva V, Hubert J. Whole genomic sequencing and sex-dependent abundance estimation of *Cardinium* sp., a common and hyperabundant bacterial endosymbiont of the American house dust mite, *Dermatophagoides farinae*. Exp Appl Acarol. 2020;80:363–80.
44. Velegraki A, Cafarchia C, Gaitanis G, Iatta R, Boekhout T. *Malassezia* infections in humans and animals: pathophysiology, detection, and treatment. PLoS Pathog. 2015;11:e1004523.
45. Harada K, Saito M, Sugita T, Tsuboi R. *Malassezia* species and their associated skin diseases. J Dermatol. 2015;42:250–7.
46. Bond R, Guillot J, Javier Cabanes F. *Malassezia* yeasts in animal disease. In: Boekhout T, Mayser P, Gueho-Kellermann E, Velegraki A, editors. *Malassezia* and the skin. Berlin & Heidelberg: Springer; 2010. p. 271–299.
47. Nesvorna M, Bittner V, Hubert J. The mite *Tyrophagus putrescentiae* hosts population-specific microbiomes that respond weakly to starvation. Microb Ecol. 2019;77:488–501.
48. Hubert J, Nesvorna M, Sopko B, Smrz J, Klimov P, Erban T. Two populations of mites (*Tyrophagus putrescentiae*) differ in response to feeding on feces-containing diets. Front Microbiol. 2018;9:2590.
49. Smrz J. Internal anatomy of *Hypochthonius rufulus* (Acari: Oribatida). J Morphol. 1989;200:215–30.
50. Chemidlin Prevost-Boure N, Christen R, Dequiedt S, Mougel C, Lelievre M, Jolivet C, et al. Validation and application of a PCR primer set to quantify fungal communities in the soil environment by real-time quantitative PCR. PLoS One 2011;6:e24166.
51. Caporaso JG, Lauber CL, Walters WA, Berg-Lyons D, Huntley J, Fierer N, et al. Ultra-high-throughput microbial community analysis on the Illumina HiSeq and MiSeq platforms. ISME J. 2012;6:1621–4.
52. Vainio EJ, Hantula J. Direct analysis of wood-inhabiting fungi using denaturing gradient gel electrophoresis of amplified ribosomal DNA. Mycol Res. 2000;104:927–36.
53. Hanshew AS, Mason CJ, Raffa KF, Currie CR. Minimization of chloroplast contamination in 16S rRNA gene pyrosequencing of insect herbivore bacterial communities. J Microbiol Methods 2013;95:149–55.
54. Sakai M, Matsuka A, Komura T, Kanazawa S. Application of a new PCR primer for terminal restriction fragment length polymorphism analysis of the bacterial communities in plant roots. J Microbiol Methods 2004;59:81–9.

55. Naqib A, Poggi S, Wang W, Hyde M, Kunstman K, Green SJ. Making and sequencing heavily multiplexed, high-throughput 16S ribosomal RNA gene amplicon libraries using a flexible, two-stage PCR protocol. In: Raghavachari N, Garcia-Reyero N, editors. Gene expression analysis: methods and protocols. New York, NY: Humana Press; 2018. p. 149–69.
56. Earley ZM, Akhtar S, Green SJ, Naqib A, Khan O, Cannon AR, et al. Burn injury alters the intestinal microbiome and increases gut permeability and bacterial translocation. PLoS One 2015;10:e0129996.
57. Schloss PD, Westcott SL, Ryabin T, Hall JR, Hartmann M, Hollister EB, et al. Introducing mothur: open-source, platform-independent, community-supported software for describing and comparing microbial communities. Appl Environ Microbiol. 2009;75:7537–41.
58. Edgar RC. UNOISE2: improved error-correction for Illumina 16S and ITS amplicon sequencing. bioRxiv 2016. doi:10.1101/081257. https://www.biorxiv.org/content/early/2016/10/15/081257. Accessed 17 Jan 2019.
59. Edgar RC. UPARSE: highly accurate OTU sequences from microbial amplicon reads. Nat Methods 2013;10:996–8.
60. Kozich JJ, Westcott SL, Baxter NT, Highlander SK, Schloss PD. Development of a dual-index sequencing strategy and curation pipeline for analyzing amplicon sequence data on the MiSeq Illumina sequencing platform. Appl Environ Microbiol. 2013;79:5112–20.
61. Cole JR, Wang Q, Fish JA, Chai B, McGarrell DM, Sun Y, et al. Ribosomal Database Project: data and tools for high throughput rRNA analysis. Nucleic Acids Res. 2014;42:D633–42.
62. Quast C, Pruesse E, Yilmaz P, Gerken J, Schweer T, Yarza P, et al. The SILVA ribosomal RNA gene database project: improved data processing and web-based tools. Nucleic Acids Res. 2013;41:D590–6.
63. Altschul SF, Gish W, Miller W, Myers EW, Lipman DJ. Basic local alignment search tool. J Mol Biol. 1990;215:403–10.
64. Kopecky J, Nesvorna M, Mareckova-Sagova M, Hubert J. The effect of antibiotics on associated bacterial community of stored product mites. PLoS One 2014;9:e112919.
65. Hammer O. Past 3.x - the past of the future: current version (October 2018): 3.21. Oslo: Natural History Museum, University of Oslo. 2018. https://folk.uio.no/ohammer/past/. Accessed 17 Jan 2019.
66. R Core Team. R: a language and environment for statistical computing, reference index version 3.3.1. Vienna: R Foundation for Statistical Computing. 2017. http://www.R-project.org. Accessed 17 Jan 2019.
67. Oksanen J. Vegan: An introduction to ordination: processed with vegan 2.5-3 in R under development (unstable) (2018-10-23 r75481) on October 24, 2018. The Comprehensive R Archive Network; 2018. https://cran.r-project.org/web/packages/vegan/vignettes/intro-vegan.pdf. Accessed 17 Jan 2019.
68. Dray S, Bauman D, Blanchet G, Borcard D, Clappe S, Guenard G, et al. Package 'adespatial': multivariate multiscale spatial analysis (version 0.3-2, 2018-09-26). The Comprehensive R Archive

Network. 2018. https://cran.r-project.org/web/packages/adespatial/adespatial.pdf. Accessed 17 Jan 2019.

69. Wood SN. Generalized additive models: an introduction with R. 1st edn. Boca Raton, FL: CRC Press; 2006.
70. Clarke KR. Non-parametric multivariate analyses of changes in community structure. Austral Ecol. 1993;18:117–43.

Additional Files

Additional file 1

Table S1 Oligonucleotide primers for PCR and qPCR quantification of 16S rRNA and 18S rRNA genes in *Dermatophagoides pteronyssinus* samples.

Figure S1 Comparison of the amount of guanine in the bodies of mites in the initial and declining phase of experiments. The columns are medians and bars represent interquartile range.

Figure S2 Histological observations of the gut of *D. pteronyssinus*. **A** – ingestion of unidentified diet pieces (arrows) in ventriculus; **B** – fragmented mycelium without contents in ventriculus (arrows), **C** – the undigested spores in ventriculus (arrows); **D** – detail of spores (arrows) ventriculus, **E** – detail of fragmented diet (arrows) in colon. **ACE** – 28 days, **D** – 56 days, **B** – 70 days old culture; Scales 50µ **ABC**, 25µ **D; Legend:** ca – caecum, co – colon, eo – eosophagus, v – ventriculus.

Figure S3 Heatmap of microbiomes of the *D. pteronyssinus* samples during the mite culture growth, **A** – bacterial and **B** – fungal community. Samples of ingested microbial community are indicated by black color, while red color indicates samples from the mite culture environment.

Figure S4 Quantification of the microbial composition in the ingested and environmental communities of *D. pteronyssinus* culture during the mite culture growth using qPCR. Copy number was estimated by amplification using universal and taxon-specific primers (Table S1), and data were recalculated on a per mite (ingested microbial community) or per gram of diet (environmental community) basis.

Figure S5 Experimental design of the study.

Additional file 2

Supplementary datasets in MS-Excel

Table S2 Samples and accession numbers in the SRA database, project PRJNA534281.

Table S3 Identification of bacterial OTUs based on GenBank data.

Table S4 Identification of fungal OTUs based on GenBank data.

Table S5 Standardized bacterial reads identified in *Dermatophagoides pteronyssinus* cultures.

Table S6 Standardized fungal reads identified in *D. pteronyssinus* cultures.

Table S7 Respiration of microcosms of *D. pteronyssinus* cultures during mite culture growth.

Table S8 Population density of *D. pteronyssinus* cultures during mite culture growth.

Table S9 Guanine contents in SPGM samplers of *D. pteronyssinus* cultures during mite culture growth.

Table S10 Numbers of DNA copies amplified by universal and taxon-specific primers from *D. pteronyssinus* cultures during mite culture growth.

Table S11 Results of METSTATS analyses for internal bacterial community of *D. pteronyssinus*. The P-values indicating significant differences among sampling time are showed.

Table S12 Results of METSTATS analyses for external culture bacterial community of *D. pteronyssinus*. The P-values indicating significant differences among sampling time are showed.

Table S13 Results of METSTATS analyses for internal fungal community of *D. pteronyssinus*. The P-values indicating significant differences among sampling time are showed.

Table S14 Results of METSTATS analyses for external culture fungal community of *D. pteronyssinus*. The P-values indicating significant differences among sampling time are showed.

Figures

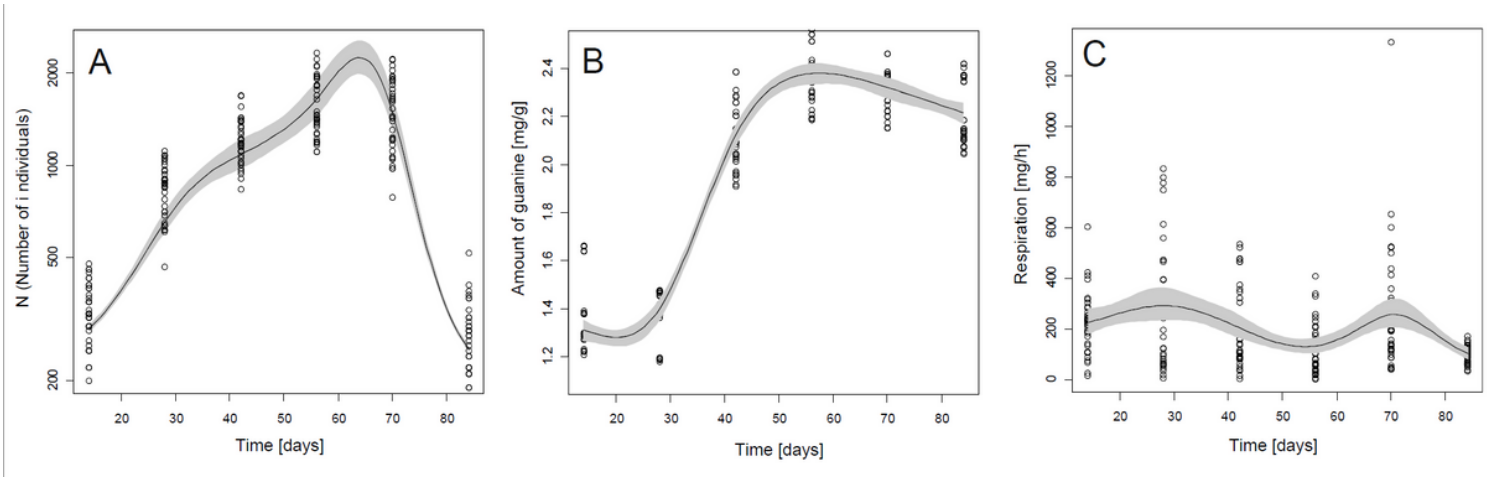

Figure 1

Changes in three main responses during culture growth of Dermatophagoides pteronyssinus. A. Number of mite individuals. B. Amount of guanine (nitrogenous waste metabolite of mites). C. Respiration of microcosms. All experiments were done over the period of 84 days, in six replicates (rearing chambers). The smoothed curves (full line) were estimated by means of GAMM. Grey bands are 95% confidence bands.

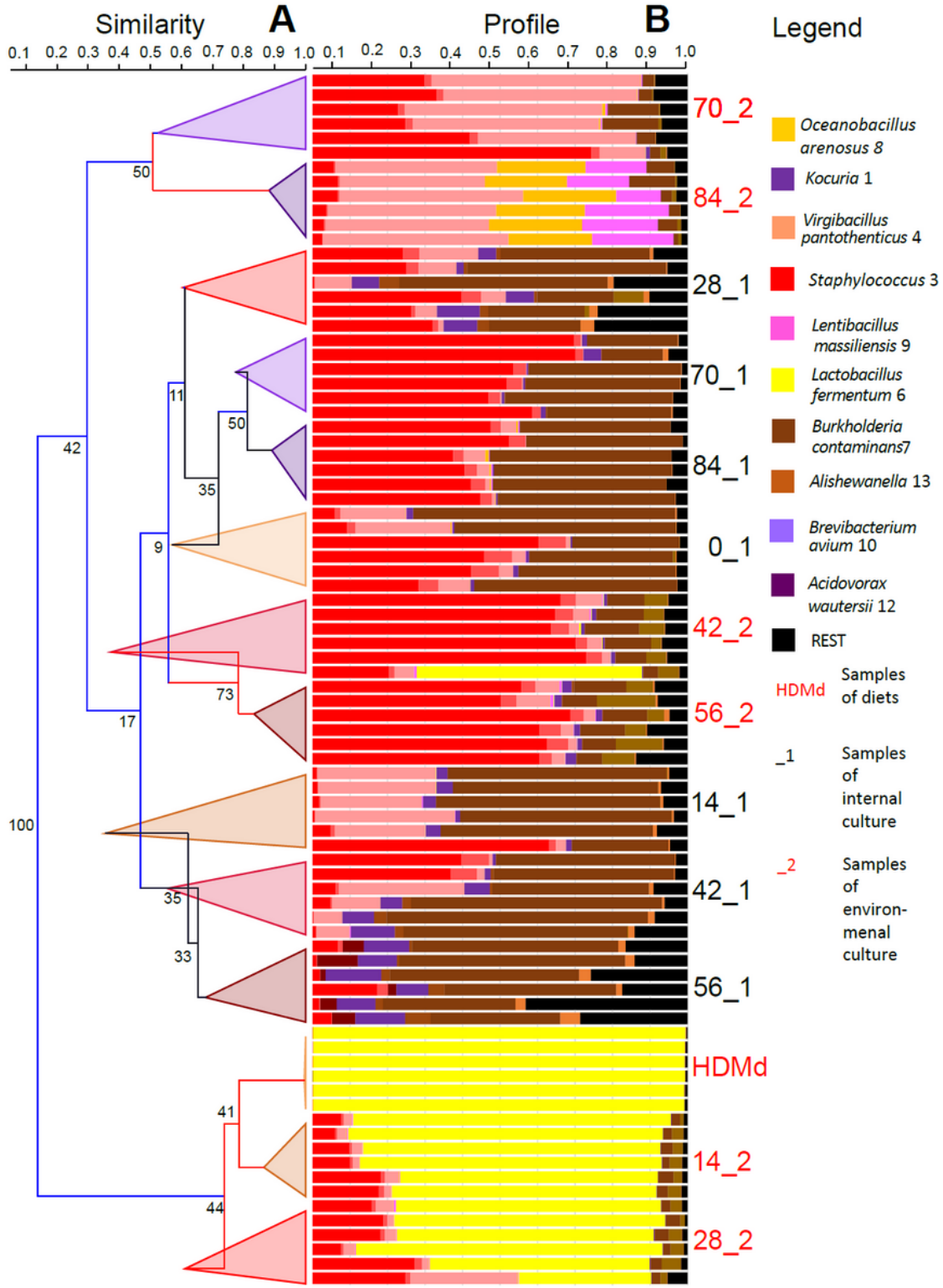

Figure 2

Changes in bacterial community profiles during the D. pteronyssinus culture growth as evaluated by barcode sequencing of internal and external community, A – the clusters based on paired group (UPGMA) clustering data in Bray–Curtis distance. The samples are grouped and triangles indicate the differences inside the samples, and the values on the branches indicate hit probability based on the bootstraps. B – the profiles of OTUs in the samples.

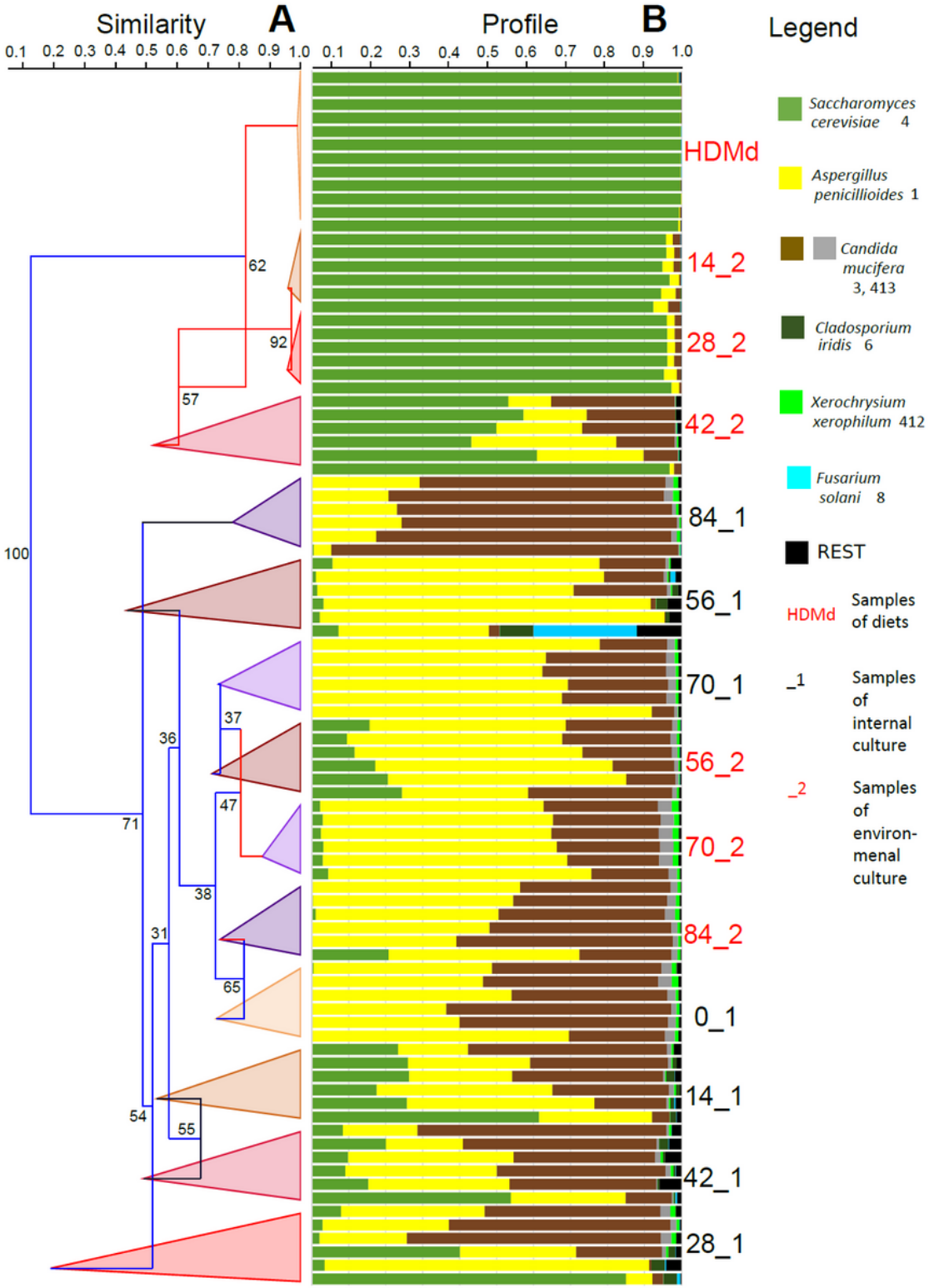

Figure 3

Changes in fungal community profiles during the D. pteronyssinus culture growth as evaluated by barcode sequencing of internal and external community, A – the clusters based on paired group (UPGMA) clustering data in Bray–Curtis distance. The samples are grouped and triangles indicate the differences inside the samples, and the values on the branches indicate hit probability based on the bootstraps. B – the profiles of OTUs in the samples.

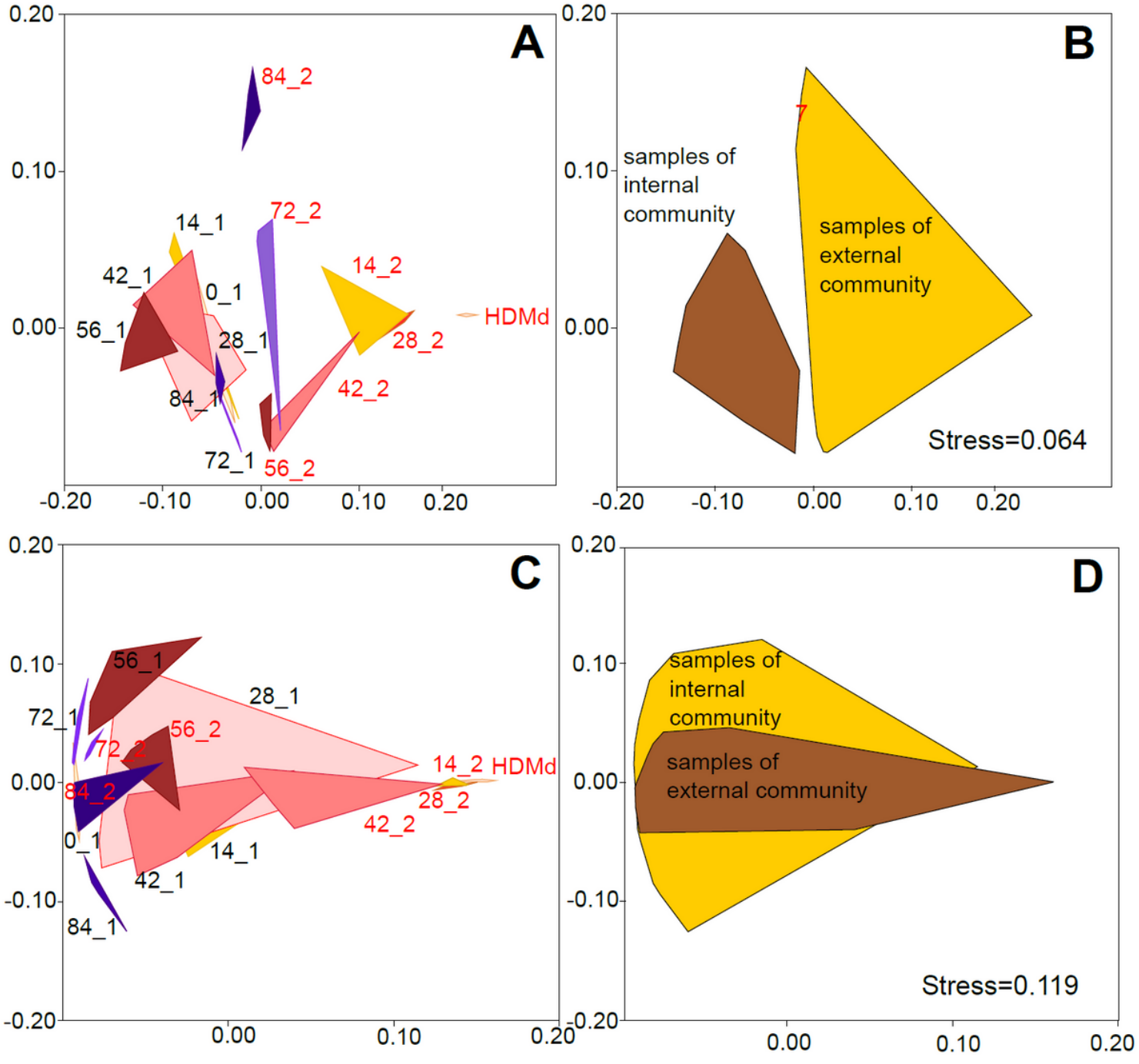

Figure 4

Non-metric multidimensional scaling of bacterial (AB) and fungal (CD) microbiome of D. pteronyssinus culture. The convex hulls are showed for different sampling times (AC). The hulls are described by

sampling times, _1 indicates internal and _2 indicates external community. The same comparison was done for and internal or external community (BD).

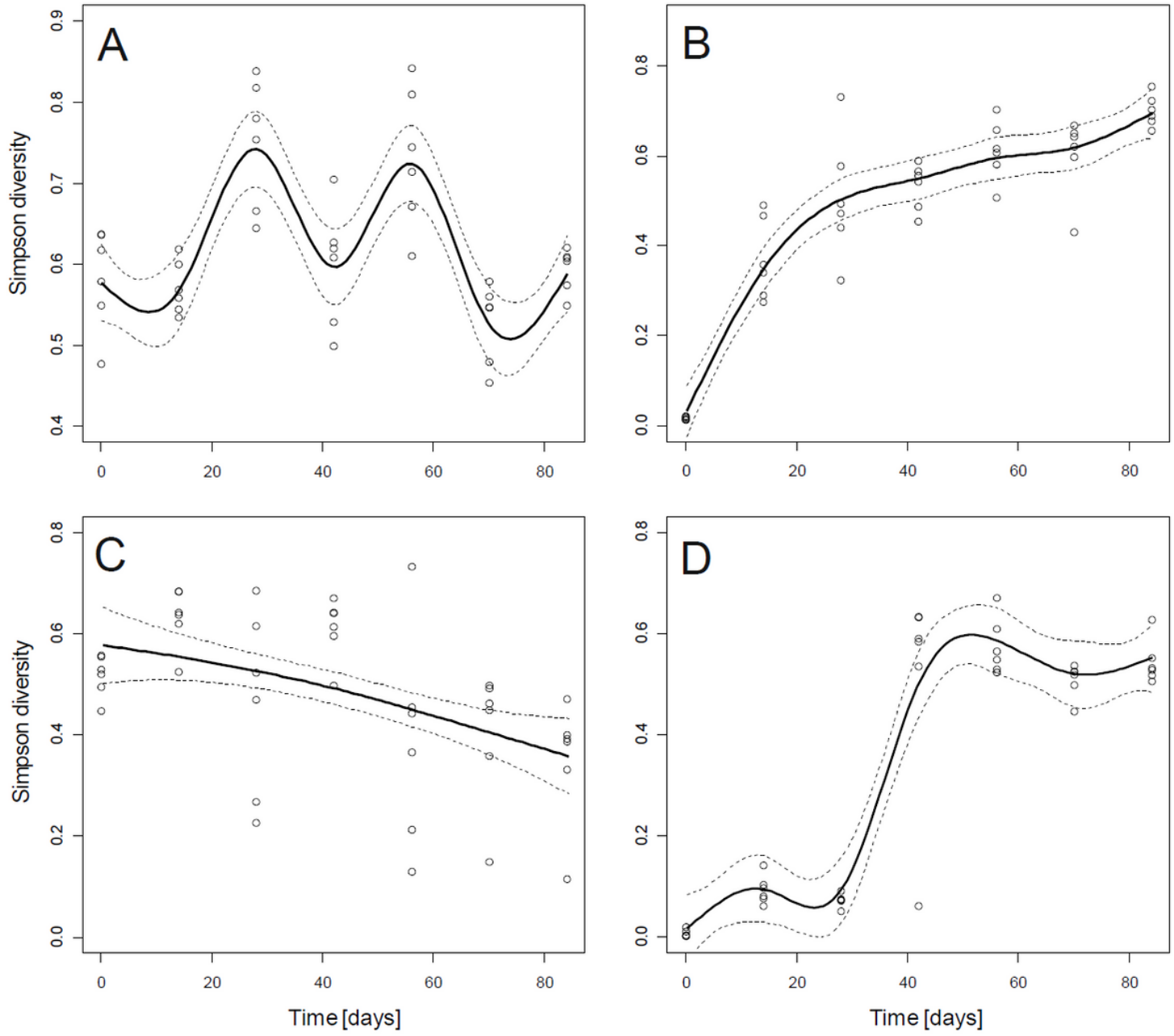

Figure 5

Changes in the alpha diversity of the microbiome of D. pteronyssinus during mite culture development. A – mite internal bacterial microbiome; B – environmental culture microbiome; C – mite internal fungal microbiome; D – environmental culture fungal microbiome. The alpha diversity was estimated by the inverse Simpson diversity index. Experiments were performed in six replicate rearing chambers. Illumina datasets were generated for each replicate and then standardized. The smoothed curve (solid line) was estimated by a GAMM, the dotted lines show 95% confidence bands.

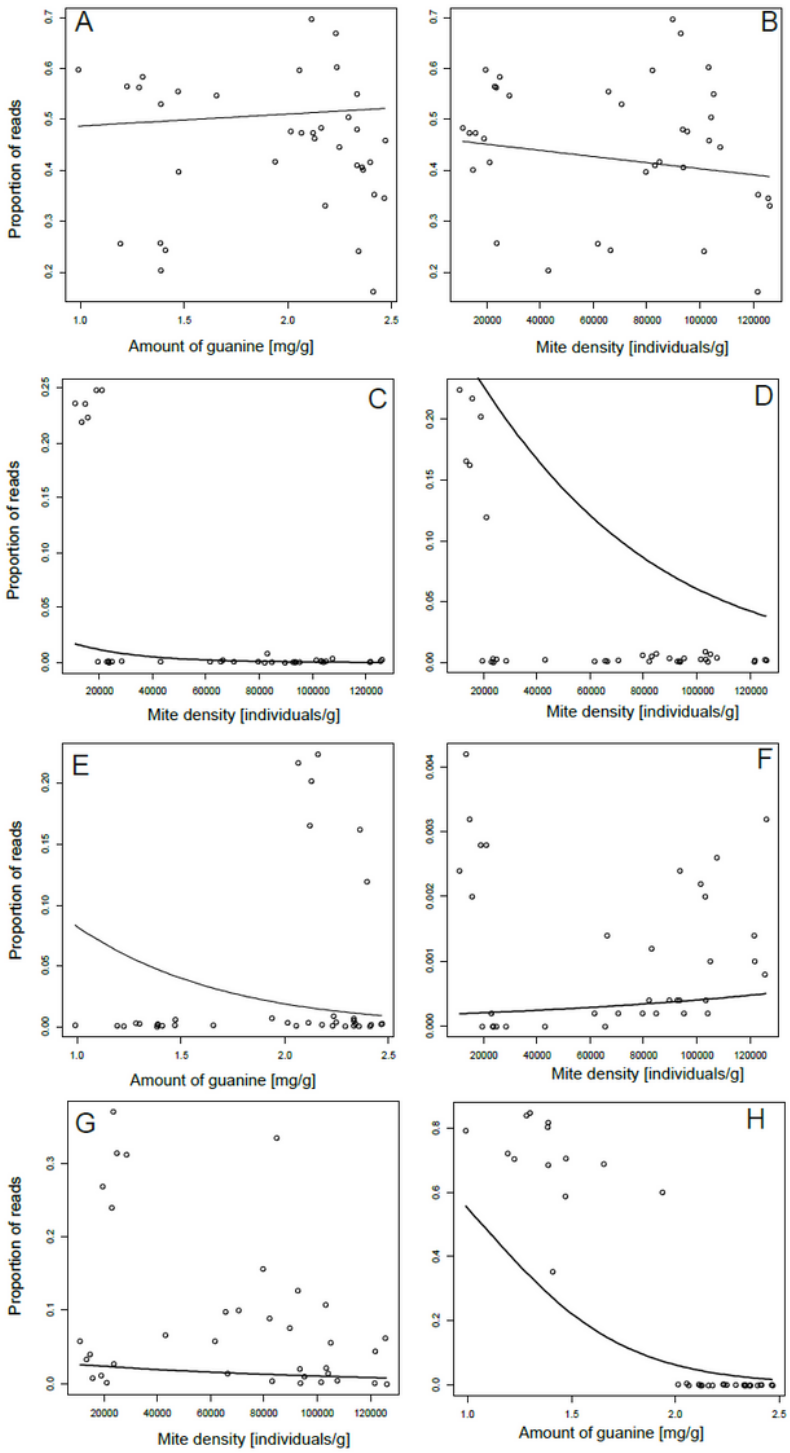

Figure 6

Relationships between the proportion of bacterial reads, mite density (A, C, D, F, G) and guanine amount (B, E. H) in mite ingested community (A, G, H) or environmental culture (B–F). A-B. OTU_1 - Kocuria. C. OTU_8 - Oceanobacillus arenosus. D–E. OTU_9 - Lentibacillus massiliensis. F. OTU_218 Bacillus sp2. G.OTU_4 Virgibacillus pantothenticus. H. OTU_6 Lactobacillus fermentum. Estimated logit curves are shown.

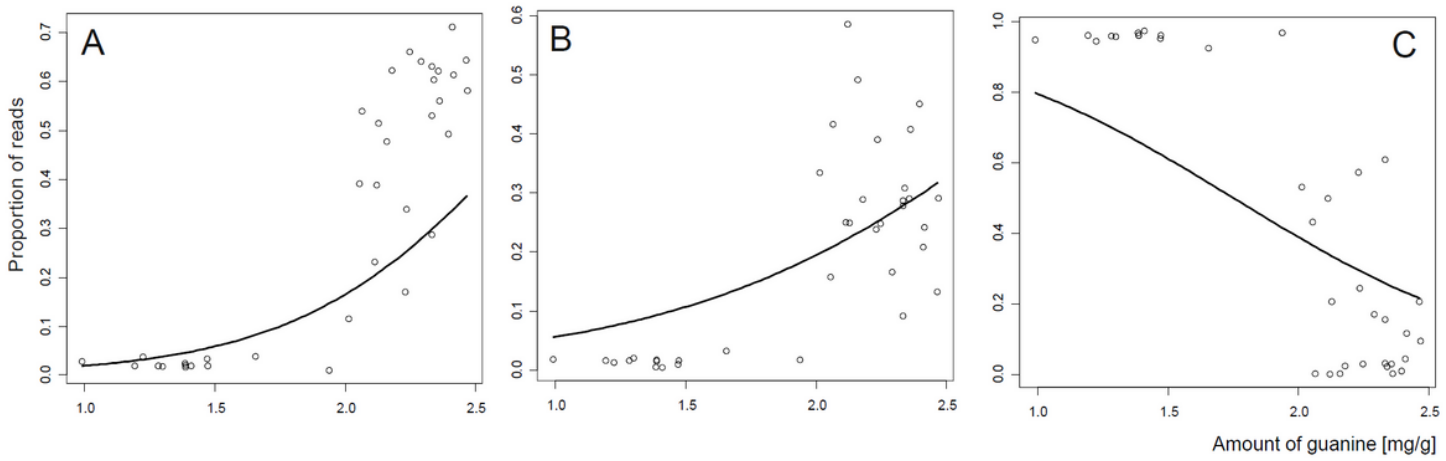

Figure 7

Relationships between the proportion of reads of fungi and guanine amount in environmental culture samples. A. FOTU_1 Aspergillus penicillioides. B. FOTU_3 Candida mucifera. C. FOTU_4 Saccharomyces cerevisiae. Estimated logit curves are shown.

Supplementary Files

This is a list of supplementary files associated with this preprint. Click to download.

- DP2019Additionalfile2R.xlsx
- DP2019Additionalfile1R.docx